JOURNAL OF AIRCRAFT
Vol. 37, No. 3, May–June 2000

Prediction of Vertical Tail Maneuver Loads Using Backpropagation Neural Networks

David Kim* and Maciej Marciniak†
Embry-Riddle Aeronautical University, Daytona Beach, Florida 32114

Federal aviation regulations require that structures critical to the safe operation of an aircraft must not fail within their expected lifetimes due to damage caused by the repeated loads typical to its operations. A backpropagation neural network has been used to predict maneuver-induced strains in the vertical tail spar of a Cessna 172P. Linear accelerometer, angular accelerometer, rate gyro, and strain gauge signals were collected during flights using a portable data acquisition system for Dutch roll, roll, sideslip, level turn, and push–pull maneuvers. Sensor signals were filtered and used to train the network. The strains in the vertical tail spar were predicted successfully by the network to within 50 $\theta\varepsilon$ of their strain gauge values. This is an inexpensive and effective technique for collecting vertical tail load spectra for small transport airplanes already in service where installation of strain gauges are impractical.

Nomenclature

c.g. Ny, Nz	= lateral and normal acceleration measured near the airplane center of gravity
F' offset	= constant added to the value of the derivative of the neuron activation function during training to prevent neuron saturation
tail Ny, Nz	= lateral and normal acceleration measured at the airplane tail cone
W_i	= weights
X_i	= input signals
Y_i	= output signals
Z_i	= hidden signals

Introduction

FEDERAL aviation regulations require that structures critical to the safe operation of an aircraft must not fail within their expected lifetimes due to damage caused by the repeated loads typical to its operations. This requirement generates the need for evaluation of fatigue life of all critical aircraft structures. To calculate the fatigue life of a given structure using this method, one must know the loading, that is, the in-service usage spectra of this structure.[1,2] For aircraft wings, associated structures, and accessories, this information is available from the Federal Aviation Administration FAA/NASA VGH (velocity, normal acceleration, altitude) study.[3] However, there is little or no comparable information for empennage flight loads of the type of airplanes included in that study. If a comprehensive in-flight load database is to be created, a large number of aircraft used in a variety of flight conditions has to be monitored. This suggests that the best system for the task is one that is easy to install and maintain. Clearly, an efficient, practical, and cost-effective method of measuring the empennage loads in aircraft is needed similar to the NASA VGH recorder that 1) can be mounted in a convenient remote location in the airplane, 2) does not require installation of strain gauges that are often impractical for airplanes already in service, and 3) is not expensive. Thus, the main focus of this paper is to find some method of relating data collected near the aircraft center of gravity to strains occurring elsewhere, for example, in the vertical tail spar.

Received 1 September 1998; revision received 1 November 1999; accepted for publication 4 November 1999.

*Professor, Department of Aerospace Engineering. Member AIAA.
†Graduate Student, Department of Aerospace Engineering.

Previous Works

The NASA VGH program was the largest and the longest running in-flight load monitoring program for general aviation aircraft. In the United States, it also represents the only comprehensive general aviation flight loads spectra program. Data for 35,286 h of operation from 95 airplanes were evaluated and presented as part of a fatigue evaluation method for wings in the FAA report AFS-120-73-2.[1] The report on the VGH project, DOT/FAA/CT-91/20,[3] was published in 1993 and focused on normal (c.g. Nz) accelerations. The need for a similar program to evaluate fatigue life of vertical aerodynamic surfaces such as fins, rudders, and winglets, was expressed by the authors of the report. Because only the accelerations near the center of gravity were measured, this project left the problem of empennage fatigue loads unaddressed. In Europe, the Netherlands is a leader in flight loads monitoring programs. Cooperation among the Dutch National Aerospace Laboratory, NLR; the Dutch national airlines, KLM; and the Fokker company resulted in a year-long in-flight tail loads monitoring program of a Fokker 100 instrumented with strain gauges.[4]

In the area of flight loads predictions, the U.S. Navy demonstrated that it is possible to predict strains at points in the structure from the flight parameters collected.[5] In this case, c.g. Nz, wing sweep angle, angle of attack, roll rate, Mach number, altitude, and weight-on-wheels indicator were used to predict strains at a point on aft fuselage of an F-14B. Another research effort by the U.S. Navy applied neural networks to predict flight loads in the main rotor blades of a helicopter.[6] The inputs to the network were load factor; longitudinal, lateral, pitch, roll, and yaw accelerations; airspeed; aircraft mass; rate of climb; rotor speed; rotor control servo position; and stabilator position. Similar work was performed at Virginia Polytechnic Institute and State University to predict the time-varying mean and oscillatory components of the tail boom bending loads and the pitch link loads.[7] For this application, the input variables were pitch rate, roll rate, yaw rate, vertical acceleration, lateral acceleration, longitudinal acceleration, longitudinal control position, and lateral control position.

Current Work

To collect the flight loads spectra from a fleet of small transport airplanes, the cost and ease of installation of the loads monitoring system is a major issue. For many of these airplanes, even a cost of U.S. $2,000 borders on being excessive. Our motivation, then, is to find the minimum set of sensors needed to accurately predict strains in the empennage structure of a small transport aircraft, the minimum threshold value of significant strains, and the correlation between sensor output and the vertical flight loads. The testbed aircraft is a Cessna 172P. The inputs to the neural networks were provided by the signals collected in-flight from the three rate gyros and three angular accelerometers about each of the aircraft axes, two linear accelerometers measuring the z-axis and the y-axis accelerations in the vicinity of the aircraft c.g., and two linear accelerometers measuring the z-axis and the y-axis accelerations in the aircraft tail cone. The aircraft also had sensors for airspeed, altitude, and strain gauges on primary structures.

Background

Artificial neural networks are information processing systems that attempt to emulate some of the processing characteristics of the human brain. Much like its biological counterpart, an artificial neural network consists of a large number of heavily interconnected simple processing elements. This brainlike organization gives the neural network parallel processing and learning capability that is adept in solving tasks that are very difficult to accomplish using traditional computer programs. Most neural networks, like the human brain, require iterative feedback training. Depending on the task at hand, either supervised or unsupervised training is needed. Supervised training means that the neural network is given a set of input-correct output pairs to train on. Unsupervised training means that the network is only given the input data to train on. In general, prediction problems are better handled by supervised training. Neural networks are often viewed as blackboxes because, often, there is no easy way of tracing or mathematically representing the internal processes occurring within the network. This is particularly true for complex problems. Also, finding the right arrangement of processing elements for a given problem usually involves significant amounts of trial and error because there is no systematic method presently available for determining this information a priori.

Neural networks have two main components: the processing elements and the connections between them. The processing elements, sometimes called neurons or nodes, function as information processors, and the connections function as information storage. Figure 1 shows a processing element with connections going in and out of it. Each processing element first calculates a weighted sum of the input signals, then applies a transfer function to this sum and outputs the result. Transfer functions are generally nonlinear and are used to solve nonlinear problems.

Nodes within a network are arranged in layers. A typical neural network consists of an input layer, a hidden or processing layer, and an output layer. The input layer is where the initial data enter the network. The hidden layer is where most of the processing takes place. If the complexity of a given problem is high, more hidden layers may be required. Finally the output layer yields the desired information.

The neuron arrangement of the network shown in Fig. 2 is typical of a backpropagation neural network. A three-layer neural network with one layer of hidden units in the feedforward phase is shown. During the backpropagation phase of learning, signals are sent in

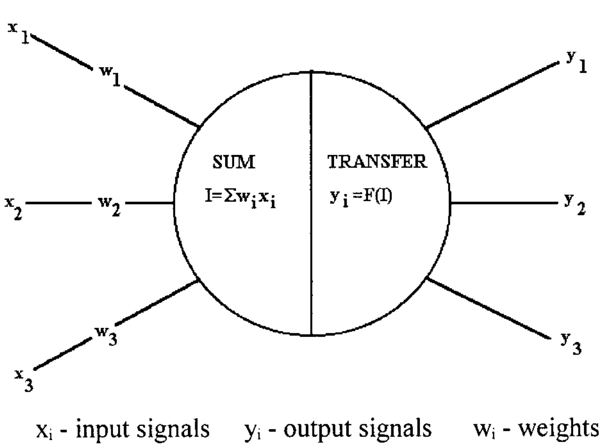

Fig. 1 Processing element.

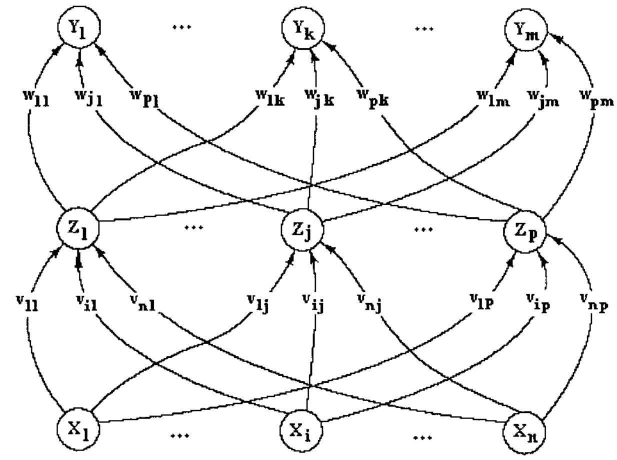

Fig. 2 Three-layer neural network.

the reverse direction. The name backpropagation comes from the training method used during the learning process, back propagation of error. This training method is simply a gradient descent method that minimizes the total squared error of the output computed by the net.

Experimental Apparatus

A specially instrumented Cessna 172P aircraft was used to collect the flight loads data. Two Columbia Research Model 2681 strain sensors were located on the front spar of the vertical tail. Two Columbia Research SA-107BHP linear accelerometers were mounted to the tail cone bulkhead to provide acceleration measurements in the empennage. The remaining two linear accelerometers (same type) were located in the cabin of the aircraft to provide acceleration measurements of the aircraft c.g. Three Murata Gyrostar ENV-05H-02 solid-state rate gyros and three Shaevitz angular accelerometers were installed in the baggage compartment on a removable instrument pallet. One rate gyro and one angular accelerometer were provided for each of the aircraft major axes: x, y, and z. The rate gyros and the angular accelerometers were added to provide a more direct measurement of the necessary kinematic variables because previous investigations by the authors showed that exclusive use of the linear accelerometers was not sufficient to predict the empennage flight loads for small airplanes with the desired accuracy. These kinematic variables were used as inputs to the neural networks. The signals from the sensors were collected by an IOTech DaqBook 216 portable data acquisition system. The DaqBook 216 was equipped with an IOTech DBK 15 universal current/voltage input card and an IOTech DBK 43 strain gauge module. The DBK 15 card was used to collect the linear accelerometer, rate gyro, and angular accelerometer signals, whereas the DBK 43 card collected data from the strain gauges. A portable computer was used to record the data during flight. Figure 3 shows the locations of the sensors and the data acquisition system in the aircraft.

Testing Procedure

The data were acquired in-flight from a series of maneuvers performed at an altitude of 3000 ft. Straight and level flight was chosen for the baseline, and the strain sensors were adjusted to output 0.0 V for this condition. Sensor readings were recorded for sideslip-left, sideslip-right, roll, push–pull, stabilized-g left turn, stabilized-g right turn, and Dutch roll maneuvers. Each maneuver was performed at 65, 80, and 95 KIAS (indicated airspeed in knots). A maximum load factor of 3.0 gk was reached during the push–pull maneuver. The maneuvers and the speeds at which they were performed were chosen to cover the full range of aircraft motions and a sizable portion of its flight envelope. The part of the flight envelope that was covered (Fig. 4) was judged to be sufficient for the purpose of establishing a method of strain prediction. Two data sets were recorded: one intended for the training of the neural networks and one for the testing. These two data sets were recorded on different

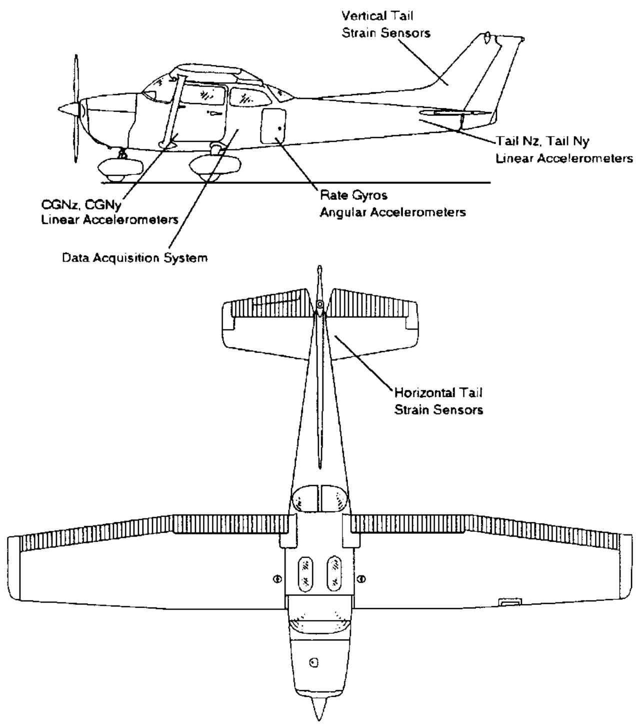

Fig. 3 Location of the sensors and the data acquisition system.

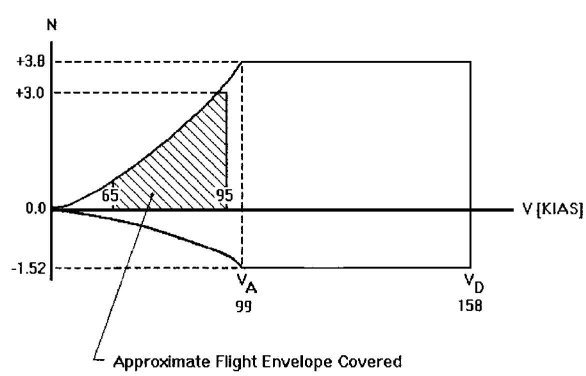

Fig. 4 Approximate flight envelope covered.

days to provide differing flight conditions. In addition, a separate file containing a typical flight profile that may be encountered by a general aviation aircraft was recorded. This file contained a climb simulating the initial climb after takeoff, a variety of turns, altitude changes and velocity changes performed in no particular order and at a wide range of airspeeds, and a descent and airspeed decrease simulating the approach to a landing. This file was recorded to determine how well the neural networks would generalize from the carefully staged training data when presented with the data that may be collected during a typical flight.

Postprocessing

Preliminary neural network results indicated that the prediction accuracy improved when the raw data was filtered prior to training the network. A frequency spectrum analysis was performed using DADisp 4.0. It indicated that the signals resulting from the pilot control inputs had frequencies of 1.5 Hz or less. Therefore, a low pass filter with a 2-Hz cutoff frequency was used with DADisp.

Neural Network Selection

The two sets of the filtered data files formed the pool of possible inputs for the neural networks. Of the two data sets, one was used for training and the other was reserved for testing. Signals recorded for the prediction of the strain in the vertical tail were c.g. and tail Ny, roll and yaw accelerations, and roll and yaw rate. For the neural networks to learn properly the relationship between the strains and the kinematic variables, the full range of measured strains had to be represented within the training files. Table 1 shows the strains measured in-flight for each maneuver. Maximum strains in the vertical tail occurred during roll and Dutch roll maneuvers.

Table 1 Maximum and minimum strains observed for each maneuver

	Vertical tail	
Maneuver	Maximum strain $\mu\varepsilon$	Minimum strain $\mu\varepsilon$
Dutch roll	165	−178
Roll	29	−119
Sideslip left	4	−92
Sideslip right	17	−68
Stabilized-g turn left	14	−69
Stabilized-g turn right	4	−71
Push–pull	−5	−61

The choice of a neural network type was driven by the relationship between the kinematic variables and the strain being unknown and there was no guarantee of this relationship remaining constant throughout the test flight envelope. In fact, a careful analysis of the flight-test data clearly shows that such relationship does not remain constant. For example, during a typical sideslip maneuver, the rudder is deflected and the resulting side load on the vertical tail creates the sideslip condition that results in a set of sensor readings. On the other hand, if the airplane is rolled abruptly with ailerons only, the dynamics of the side load induced on the vertical tail is quite different from that of side load induced by the rudder. Different sensors (kinematic variables) play the dominant role, and associated time phases are different. To cope with these variations, a modular neural network (MNN), described in detail in Ref. 8, was chosen to handle the problem. An MNN may be thought of as a generalization of the backpropagation neural network. It consists of a group of neural networks, referred to as local experts, competing to learn different aspects of a problem. A gating network controls the competition and learns to assign different regions of the data space to different local expert networks. Thus, if the relationship between the strain and the kinematic variables changed from one maneuver to another or from one speed to another, the neural network would still be able to learn to predict strain for any flight condition.

Neural Network Implementation

All of the neural networks created in the course of this research were formed, trained, and tested using the NeuralWorks Professional II+ version 5.20 software. This program is capable of automatically generating an MNN from the specified parameters. The parameters of the networks selected are listed in Table 2.

In the search for the best signals to use for training of the neural networks, the number of input layer neurons varied from two to six as various combinations of inputs were tried. The number of neurons in the hidden layer of each local expert was arbitrarily set to 30. During initial testing this number was increased to as high as 50 with no appreciable change in network performance. All local experts had a single neuron in their output layers; this was dictated by each of these networks being expected to predict a single value, the strain in the vertical tail.

The number of neurons in the hidden layer of the gating network was set to 400. Gating networks with less than 400 hidden layer neurons were tried, but the network performance decreased substantially. The number of the neurons in the output layer of the gating network (and subsequently the number of local experts) was set to five. This proved sufficient inasmuch as none of the subsequently trained networks required the use of more than three of the five available local experts.

The extended delta-bar-delta (EDBD) learning rule was selected. This learning rule automatically selected and adjusted the learning coefficient, the learning coefficient ratio, the learning coefficient

Table 2 Parameters of the MNNs

Number of inputs	Dependent on the combination of signals used for input
Local expert hidden layer neurons	30
Local expert output layer neurons	1
Gating network hidden layer neurons	400
Gating network output layer neurons	5
Learning rule	EDBD
Transfer function	Tanh
Epoch	Vertical tail network: 20
F' offset	0.3

transition point, and the momentum term. This minimized the learning time and reduced the number of network parameters that had to be selected iteratively. The hyperbolic tangent transfer function was chosen for the problem, and input values were normalized and ranged from -1 to $+1$.

The epoch sets the number of training pairs that are presented to the network before the weights are updated. Larger and smaller epochs were tried for both networks, but resulted in generally worsened network performance.

The F' offset is a constant added to the value of the derivative of the neuron activation function during training to prevent neuron saturation. The NeuralWorks users guide suggests that it be set to 0.3 for a tanh activation function. F' offsets of 0.1 and 0.2 were also tried with no change in the results.

Results

Before the results can be evaluated, one must first establish a baseline definition of the ideal neural network output. In view of the problem at hand, the following guidelines were derived. First, not all stresses that may be experienced by a structure significantly contribute to the accumulated fatigue damage. A stress lower than that necessary to cause failure after 10^7 cycles (for a given stress ratio) is not considered to cause fatigue damage. Thus, an insignificant stress region, less than 1000 psi, was conservatively defined to exist well below the Al 2024 endurance limit stress (the material for C172P vertical tail spar is Al 2024).

Second, within the significant stress region, a tolerance band of $\pm 50\ \mu\varepsilon$ was adopted. Because eventually this method is to be used to evaluate the fatigue life of empennage structures, the stresses should be predicted at least as accurately as they are plotted on the maximum stress axis of the S-N (stress vs cycle) curves. The stresses in the S-N curves found in the Military Handbook MIL-HDBK-5E are plotted to within 1000 psi, that is, the scatter of the data for S-N curves is 2000 psi or greater. For Al 2024, 1000 psi corresponds to 100 $\mu\varepsilon$. Thus, the tolerance band was selected conservatively to be $\pm 50\ \mu\varepsilon$.

The results of the vertical tail strain prediction are summarized in Table 3 and Figs. 5–8. The neural network that produced these results was trained using y- and x-axes angular accelerometer signals collected from roll and Dutch roll maneuvers, both at 80 KIAS. In the portion of the flight envelope covered during the data collection, the only maneuver that produced significant stresses in the vertical tail was the Dutch roll. Surprisingly, steady-state maneuvers, that is, sideslips, resulted only in relatively small strains. The neural network predicted 100% of the significant strains to within the predefined tolerance band. With the exception of the Dutch roll, 65 KIAS, training set file, the maximum error of prediction in the significant stress region was equal to or less than $\pm 40\ \mu\varepsilon$. All of the insignificant strains resulting from the remaining maneuvers were properly predicted.

In all cases, as the magnitude of the strains increased, the accuracy of the predictions improved. In all Dutch roll maneuvers, the largest deviation occurred in the region from -0.2 to $+0.2$ normalized measured strains. The strains of these magnitudes were observed when the aircraft was at bank and yaw angles close to 0 deg. During this portion of the maneuver, the only control input was rudder deflection, and for a short time the aircraft motion was similar to a sideslip. Thus, for the strains collected in this segment of the Dutch

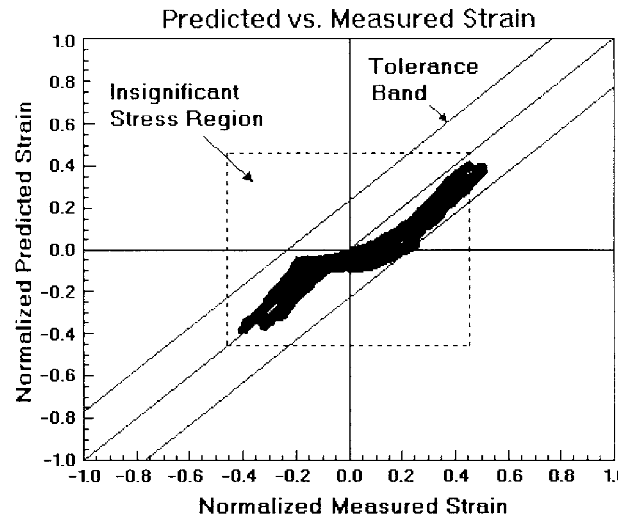

Fig. 5 Dutch roll, 65 KIAS, vertical tail, testing set: strain prediction results.

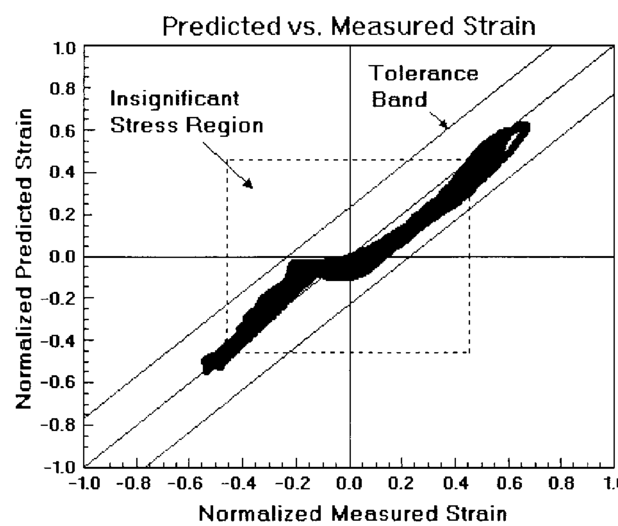

Fig. 6 Dutch roll, 80 KIAS, vertical tail, testing set: strain prediction results.

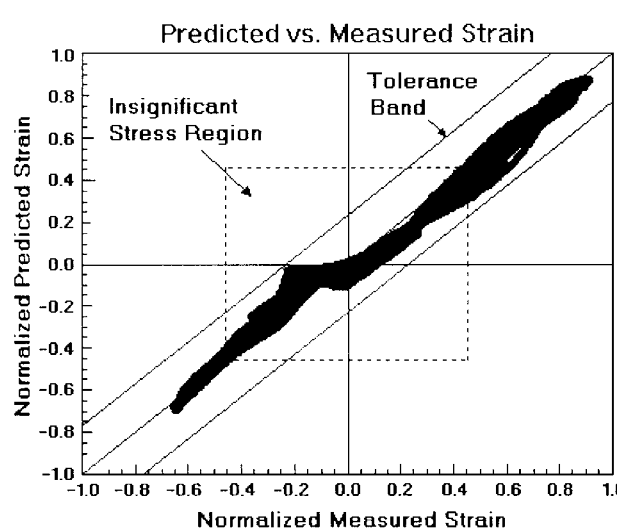

Fig. 7 Dutch roll, 95 KIAS, vertical tail, testing set: strain prediction results.

Table 3 Summary of the results of the vertical tail strain prediction

	Significant stress region		Entire data file	
Maneuver Dutch roll, KIAS	% Records outside of tolerance band	Maximum error of prediction $\mu\varepsilon$	% Records outside of tolerance band	Maximum error of prediction $\mu\varepsilon$
65, training set	0.6	51	4	51
80, training set	0	33	0	34
95, training set	0	23	0	39
65, testing set	0	34	3	51
80, testing set	0	33	0	39
95, testing set	0	34	0.3	42

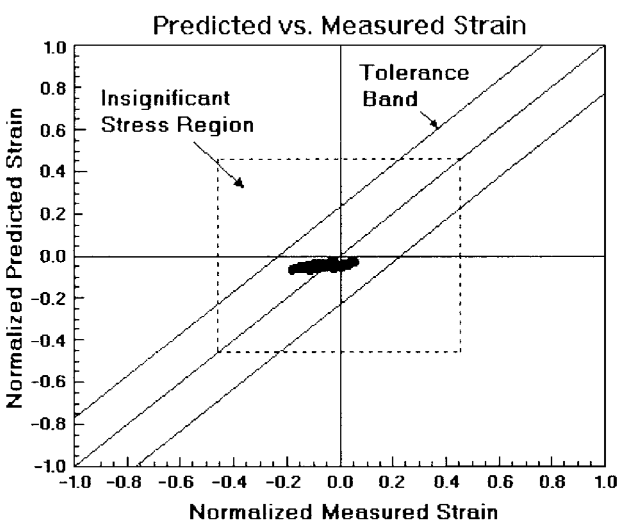

Fig. 8 Sideslip left, 80 KIAS, vertical tail, testing set: strain prediction results.

roll, the network output was very similar to that for the sideslip maneuvers shown in Fig. 8.

Conclusions

The backpropagation neural networks successfully predicted the strain behavior that resulted from the maneuver loads in the vertical tail structure of the C172P to within 50 $\mu\varepsilon$. The x- and y-axis angular accelerometers were sufficient to train the neural networks that were used to predict the strains resulting from the maneuver loads. These sensors appear to be the minimum set of sensors required to predict the strains in the vertical tail of a small transport airplane. Although not as accurate as direct measurement using strain gauges, the remote sensors and the neural networks approach seem suitable for flight loads work. The method correctly predicts the magnitude, cycle, and the sequence of the loading, that is, the complete time trace of the maneuver-induced stress. It also has an inherent advantage that the sensor signals are far less noisy than strain gauge signals.

The neural networks developed in this paper should be optimized to reduce the amount of time necessary to calculate the strains and, if necessary, to further improve the accuracy of the prediction. The method of strain prediction developed should be verified on other aircraft models, especially those with different empennage configurations. A fleet of small transport airplanes should be instrumented with similar sensors to collect empennage flight loads spectra.

Acknowledgments

This research was supported by the Federal Aviation Administration (FAA) Technical Center under Grant 93-G-026, Thomas DeFiore, Program Manager, and Terence Barnes, FAA National Resource Specialist for Flight Loads and Aeroelasticity.

References

[1]"Fatigue Evaluation of Wing and Associated Structure on Small Airplanes," Federal Aviation Administration, Rept. AFS-120-73-2, Washington, DC, 1973.

[2]"Fatigue Evaluation of Empennage, Forward Wing, and Winglets/Tip Fins," Federal Aviation Administration, Rept. ACE-100-01, Kansas City, MO, 1974.

[3]Gabriel, E. A., DeFiore, T., Locke, J. E., and Smith, H. W., "General Aviation Aircraft—Normal Acceleration Data Analysis and Collection Project, Final Report," Dept. of Transportation, Rept. DOT/FAA/CT-91/20, Federal Aviation Administration, Washington, DC, 1993.

[4]Van Gelder, P. A., "In-Flight Tailload Measurements," *Proceedings of the 18th ICAS Congress*, AIAA, Washington, DC, 1992, pp. 1058–1066.

[5]Hoffman, M. E., "A Neural Network Prototype for Predicting F-14B Strains at the B.L.10 Longeron," NAWC Rept. NAWCADWAR-92042-60, Warminster, PA, June 1992.

[6]Haas, J. D., Milano, J., and Flitter, L., "Prediction of Helicopter Component Loads Using Neural Networks," AIAA Paper 93-1301, April 1993.

[7]Cook, A. B., Fuller, C. R., O'Brien, W. F., and Cabell, R. H., "Artificial Neural Networks for Predicting Nonlinear Dynamic Helicopter Loads," *AIAA Journal*, Vol. 32, No. 5, May 1994, pp. 1072–1077.

[8]*A Technology Handbook for Professional II+ and NeuralWorks Explorer*, NeuralWare, Inc., Technical Publications Group, Pittsburgh, PA, 1995, pp. 235–237.